

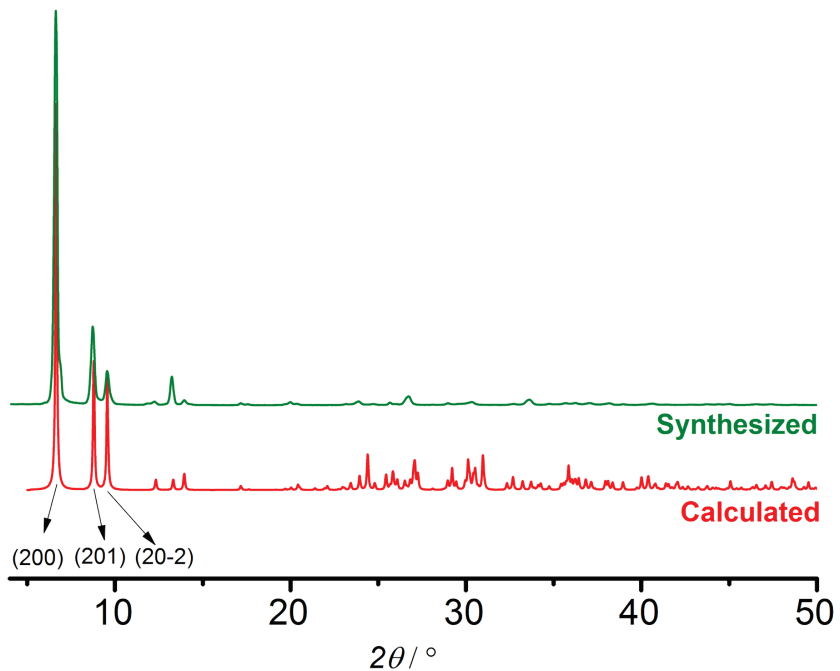
## Supporting Information

### **Flexible and luminescent fibers of a 1D Au(I)-thiophenolate coordination polymer and formation of gold nanoparticles-based composite materials for SERS**

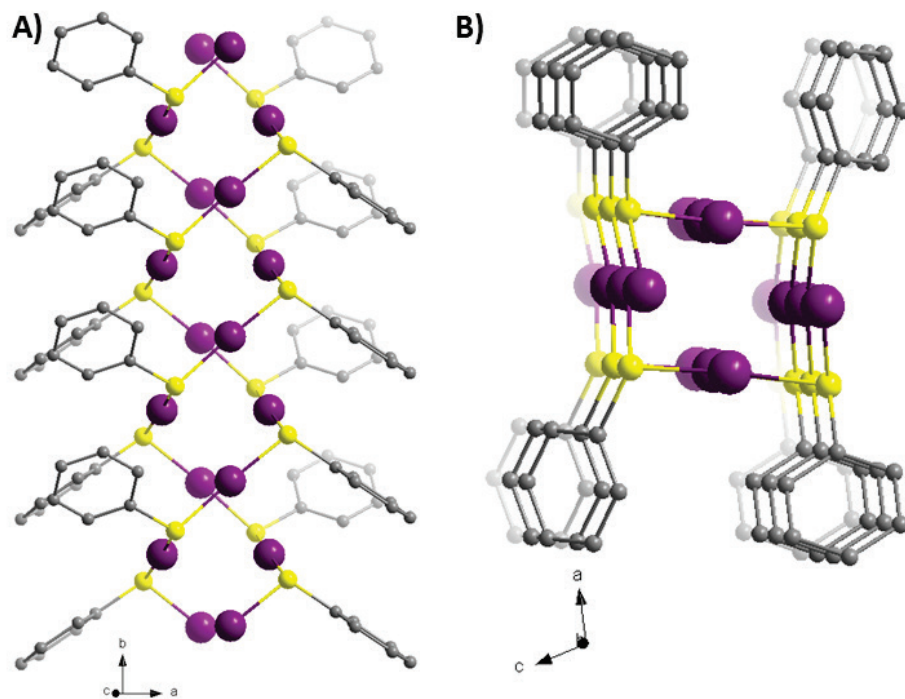
Shefali Vaidya<sup>a</sup>, Oleksandra Veselska<sup>a,b</sup>, Antonii Zhadan<sup>a</sup>, Marlène Daniel<sup>a</sup>, Gilles Ledoux<sup>c</sup>, Alexandra Fateeva<sup>d</sup>, Takaaki Tsuruoka<sup>e</sup> and Aude Demessence<sup>a\*</sup>

- <sup>a.</sup> *Univ Lyon, Université Claude Bernard Lyon 1, Institut de Recherches sur la Catalyse et l'Environnement de Lyon (IRCELYON), UMR CNRS 5256, Villeurbanne, France.*
- <sup>b.</sup> *Institute of Experimental and Applied Physics, Czech Technical University in Prague, CZ-110 00 Prague, Czech Republic.*
- <sup>c.</sup> *Univ Lyon, Université Claude Bernard Lyon 1, Institut Lumière Matière (ILM), UMR CNRS 5306, Villeurbanne, France.*
- <sup>d.</sup> *Univ Lyon, Université Claude Bernard Lyon 1, Laboratoire des Multimatériaux et Interfaces (LMI), UMR CNRS 5615, Villeurbanne, France.*
- <sup>e.</sup> *Department of Nanobiochemistry, Frontiers of Innovative Research in Science and Technology (FIRST), Konan University, Kobe, Japan.*

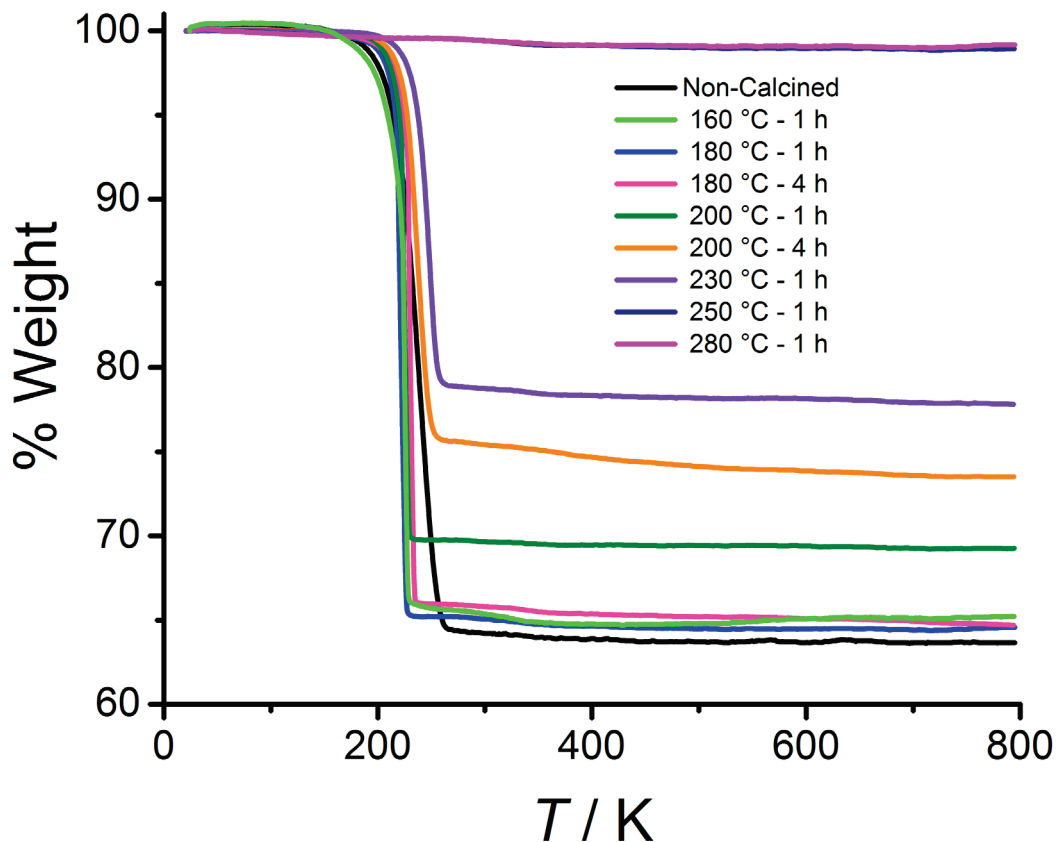
\*aude.demessence@ircelyon.univ-lyon1.fr



**Figure S1.** Powder X-Ray diffraction (PXRD) patterns of the obtained fibers compared to the calculated one of  $[\text{Au}(\text{SPh})]_n$ .



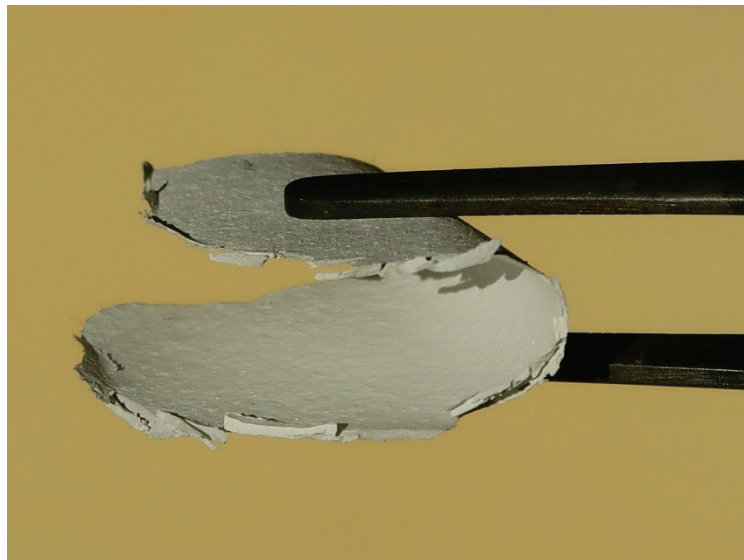
**Figure S2.**  $[\text{Au}(\text{SPh})]_n$  coordination polymer structure. View of the double helix along the A) b-axis and B) (ac) plane. Purple, Au(I); yellow, S; gray, C. Hydrogen atoms are omitted for clarity.



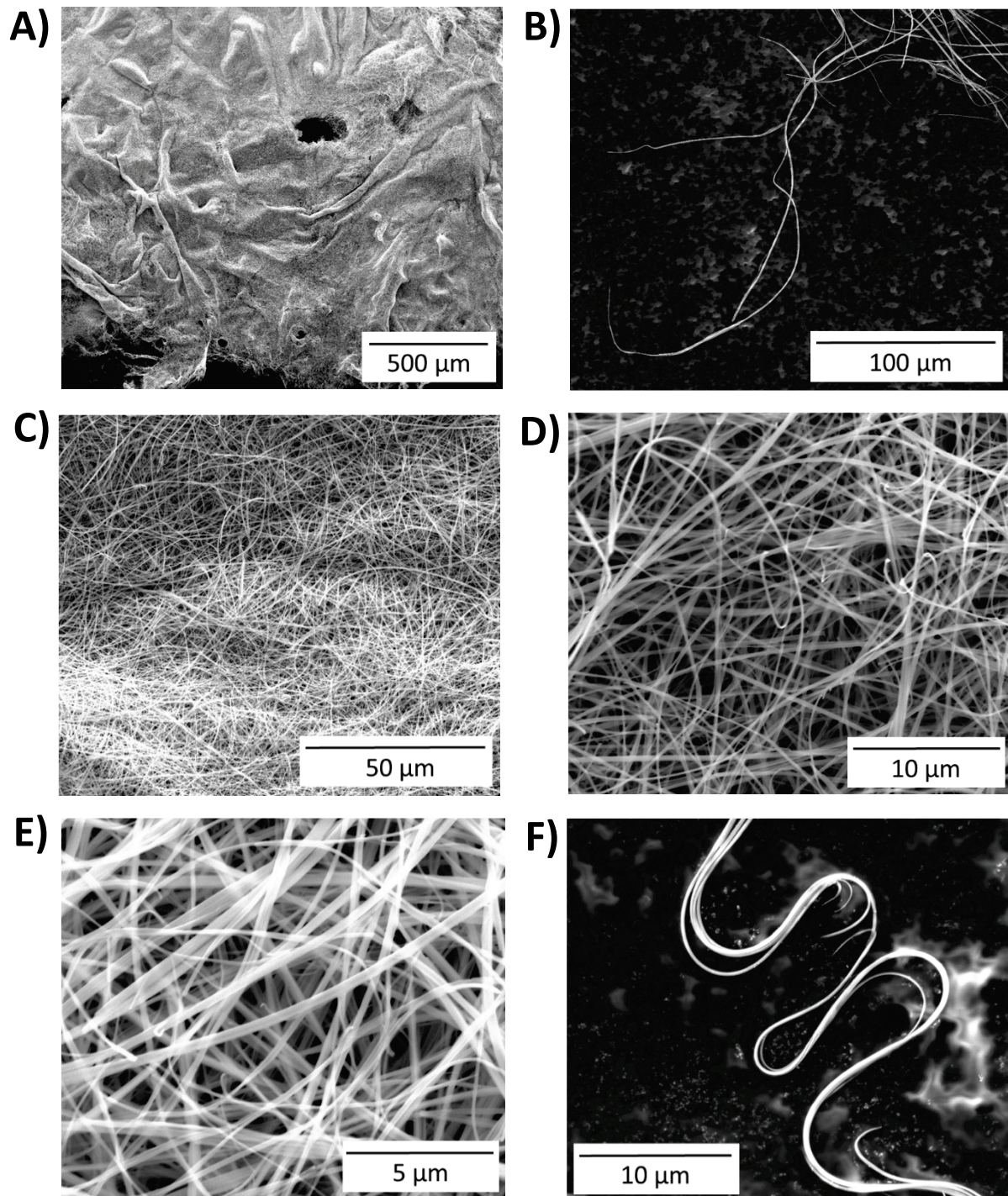
**Figure S3.** TGA (carried out under air) of  $[\text{Au}(\text{SPh})]_n$  CP and the composite materials obtained after different temperatures and times of calcination.

**Table S1.** Ligand and gold contents and the percentage of CP in the composite material obtained from TGA experiments.

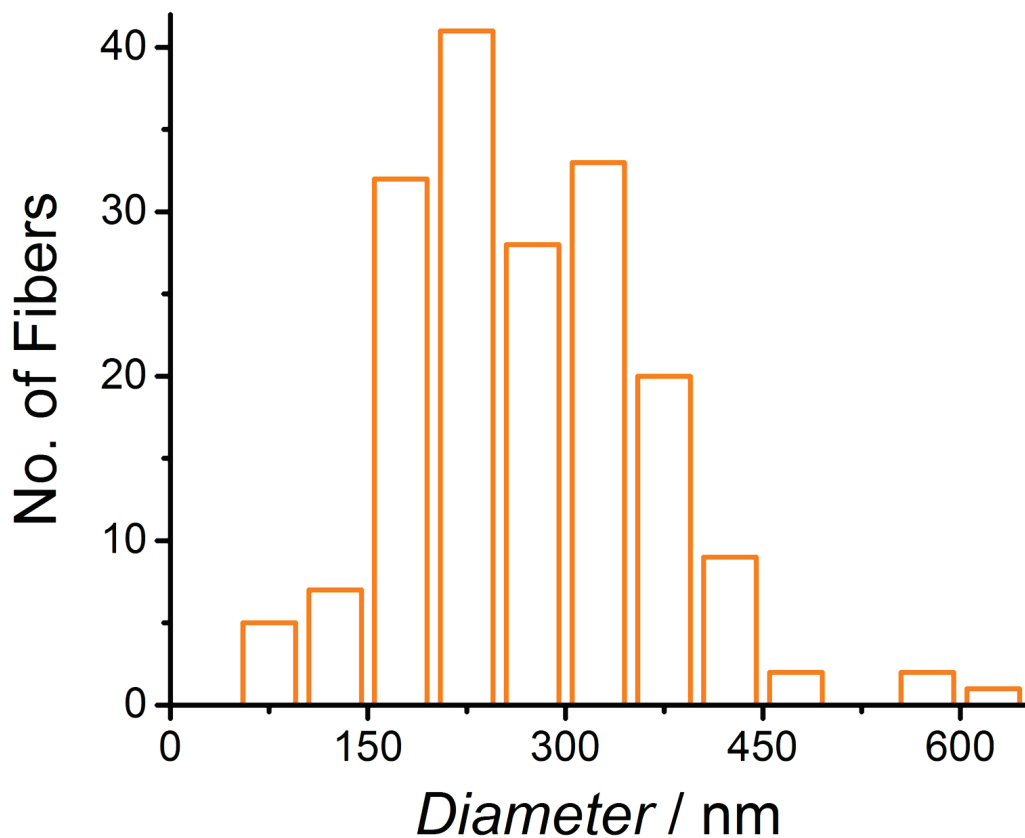
Fibers	Ligand content, %	Gold content, %	Content of CP in composite material, %
<b>Non-calcined</b>	36.0	64.0	100
<b>160 °C – 1 h</b>	35.3	64.7	98.9
<b>180 °C – 1 h</b>	35.3	64.7	98.9
<b>180 °C – 4 h</b>	35.3	64.7	98.9
<b>180 °C – 12 h</b>	35.1	64.9	98.3
<b>200 °C – 1 h</b>	30.7	69.3	86.0
<b>200 °C – 4 h</b>	26.5	73.5	74.2
<b>200 °C – 12 h</b>	21.0	79.0	58.8
<b>230 °C – 1 h</b>	23.0	77.0	64.4
<b>250 °C – 1 h</b>	1.0	99.0	2.8
<b>280 °C – 1 h</b>	1.0	99.0	2.8



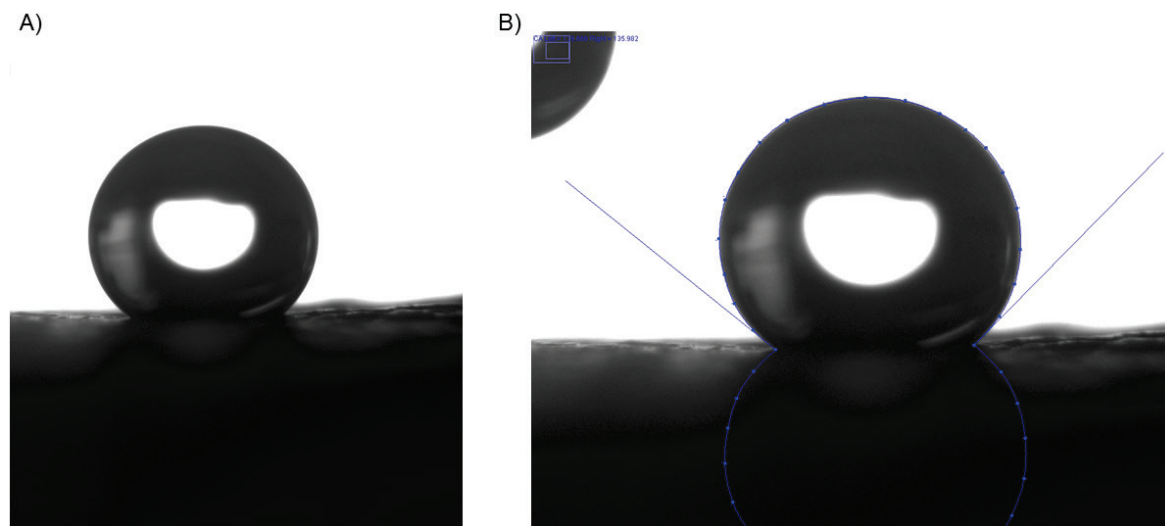
**Figure S4.** Photograph showing the flexibility of the fibers.



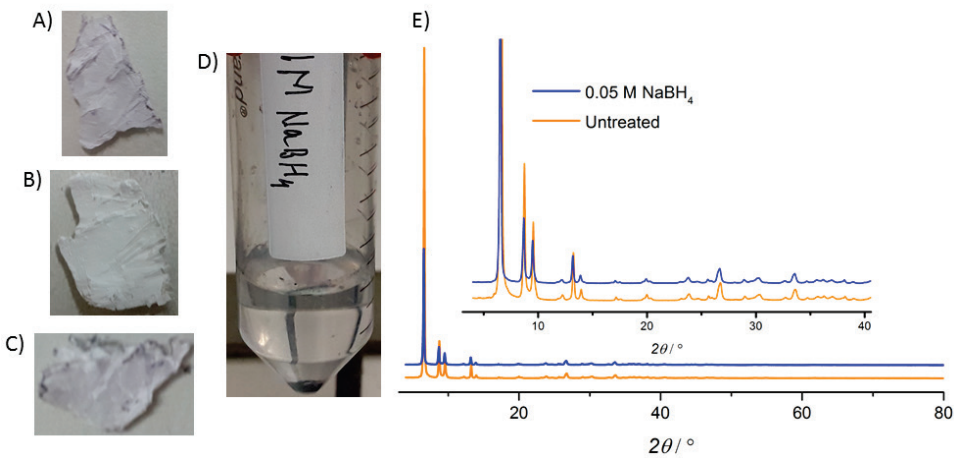
**Figure S5.** A-D) SEM images of the  $[\text{Au}(\text{SPh})]_n$  fibers at various magnification levels.



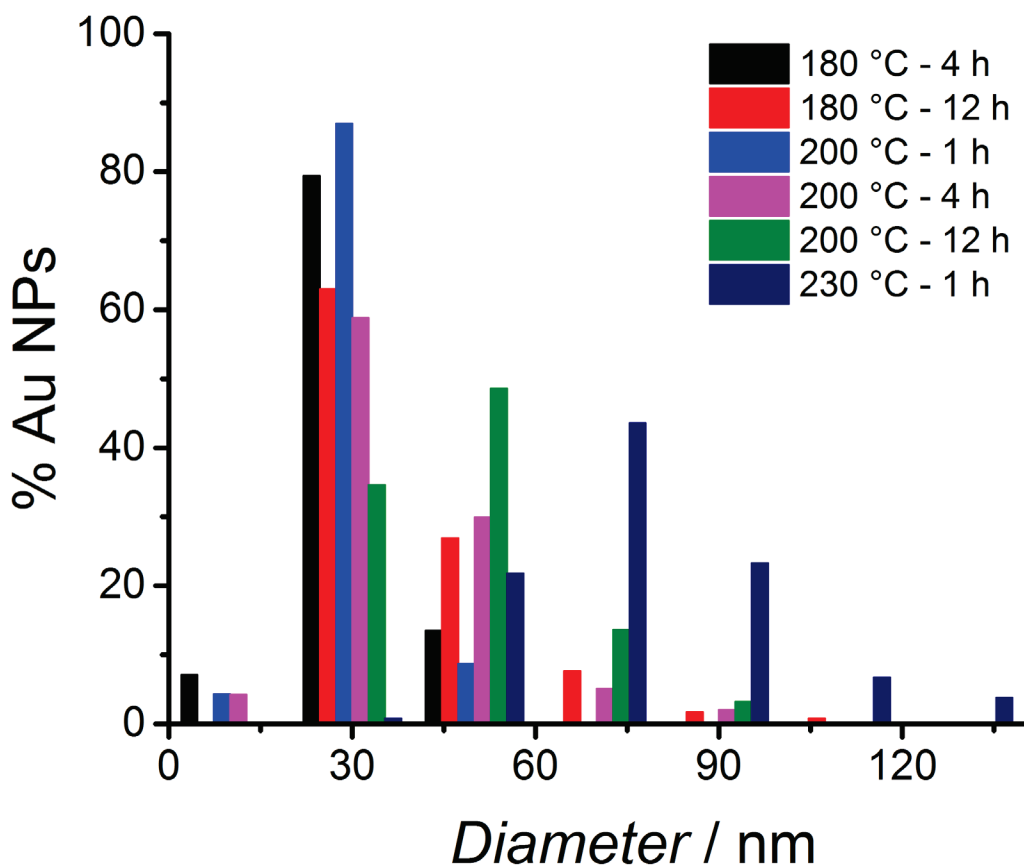
**Figure S6.** Histogram of the diameter distribution of the  $[\text{Au}(\text{SPh})]_n$  fibers measured by SEM.



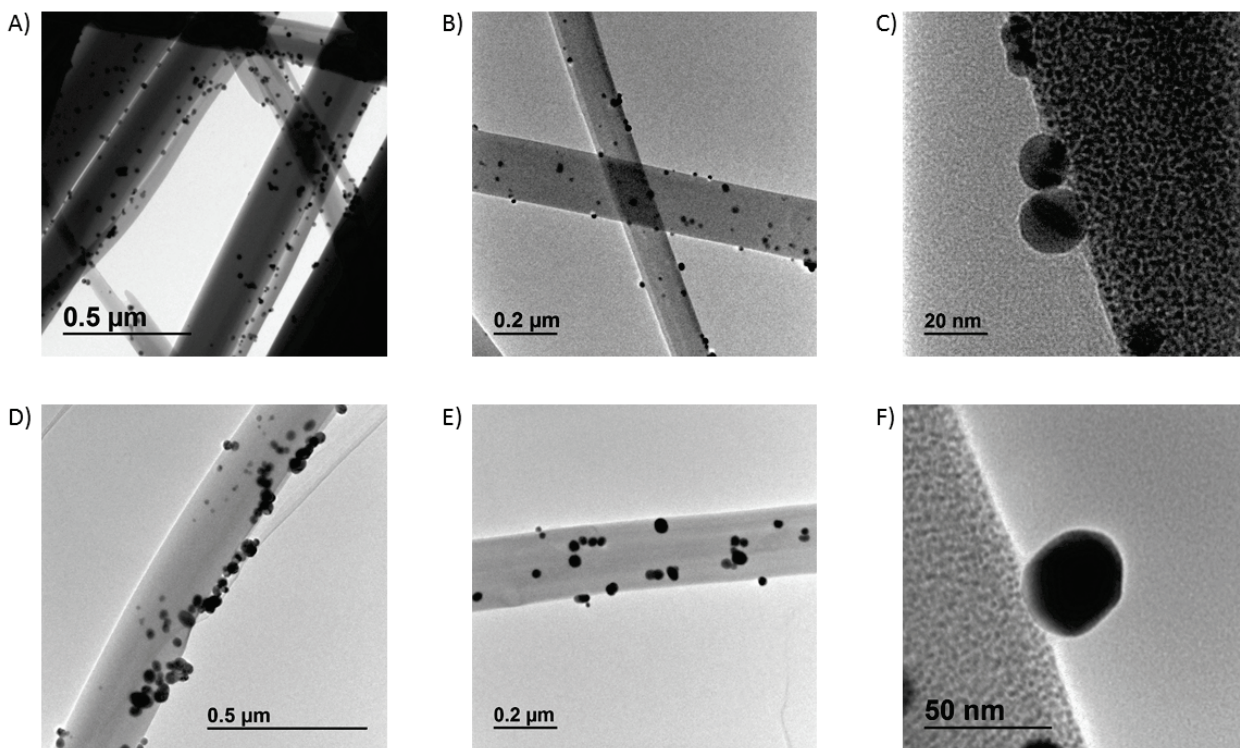
**Figure S7.** Contact angle measurement: A) and B) a droplet of water on a  $[\text{Au}(\text{SPh})]_n$  fibers film.



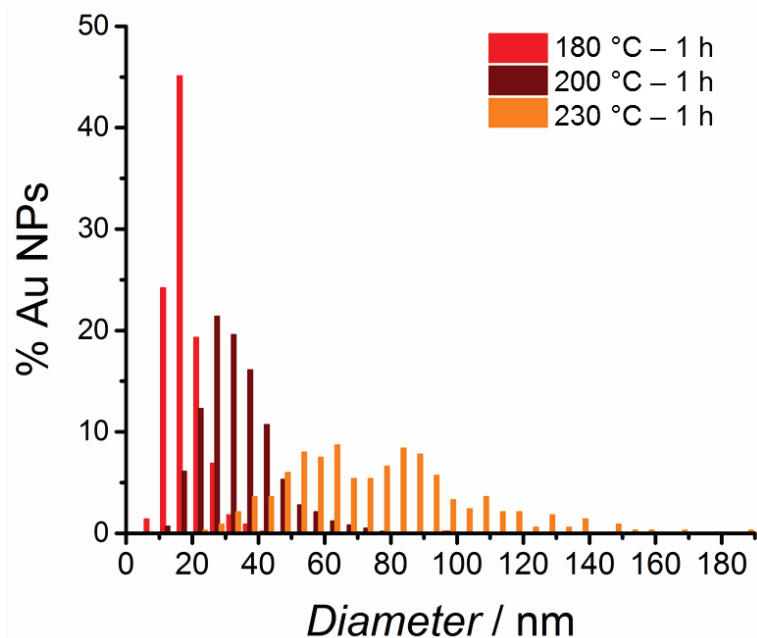
**Figure S8.** Pictures of the fibers treated with A) 10 M HCl, B) 5 M NaOH, C) 0.05 M NaBH<sub>4</sub> and D) 1 M NaBH<sub>4</sub>, resulting in the formation of a black precipitate. E) PXRD of the fibers treated with 0.05 M NaBH<sub>4</sub>.



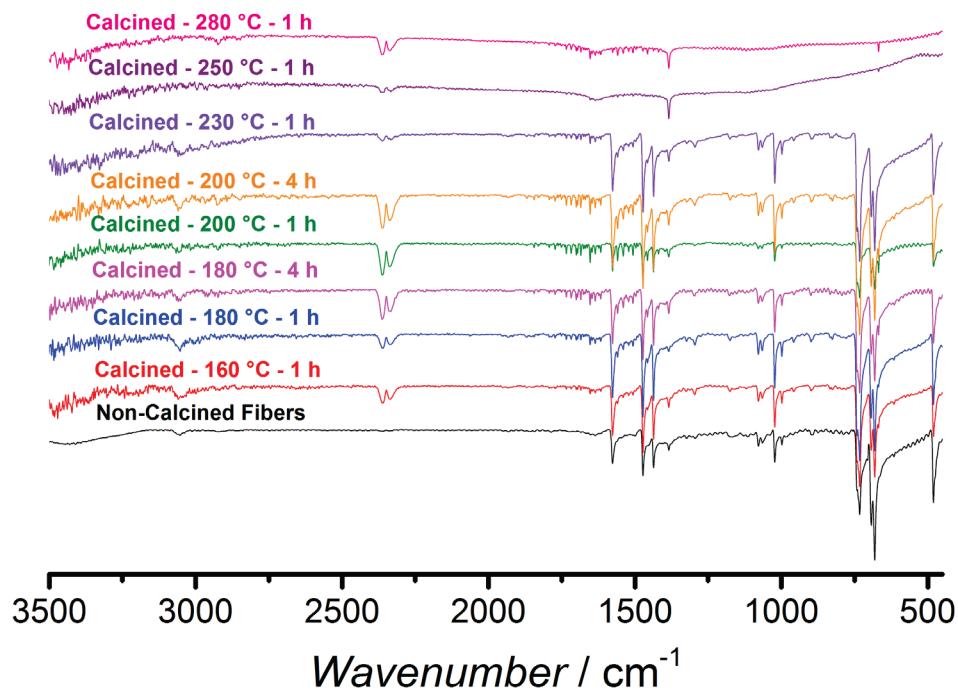
**Figure S9.** Histograms of the size distribution of the AuNPs formed on the [Au(SPh)]<sub>n</sub> fibers at various temperatures and times of calcination. The diameters are measured from SEM images.



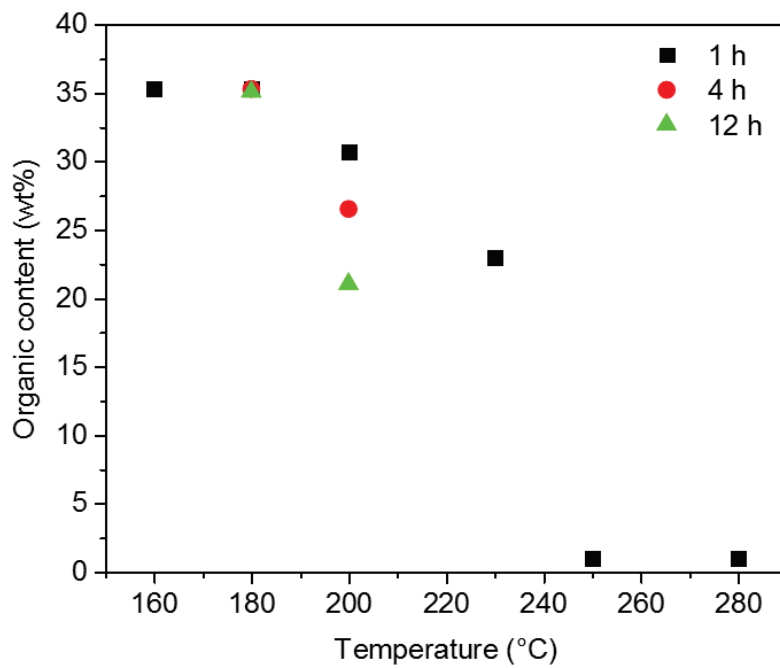
**Figure S10.** TEM images of the  $[\text{Au}(\text{SPh})]_n$  fibers calcined at A-C) 180 °C – 1 h and D-F) 200 °C – 1 h at various magnification levels.



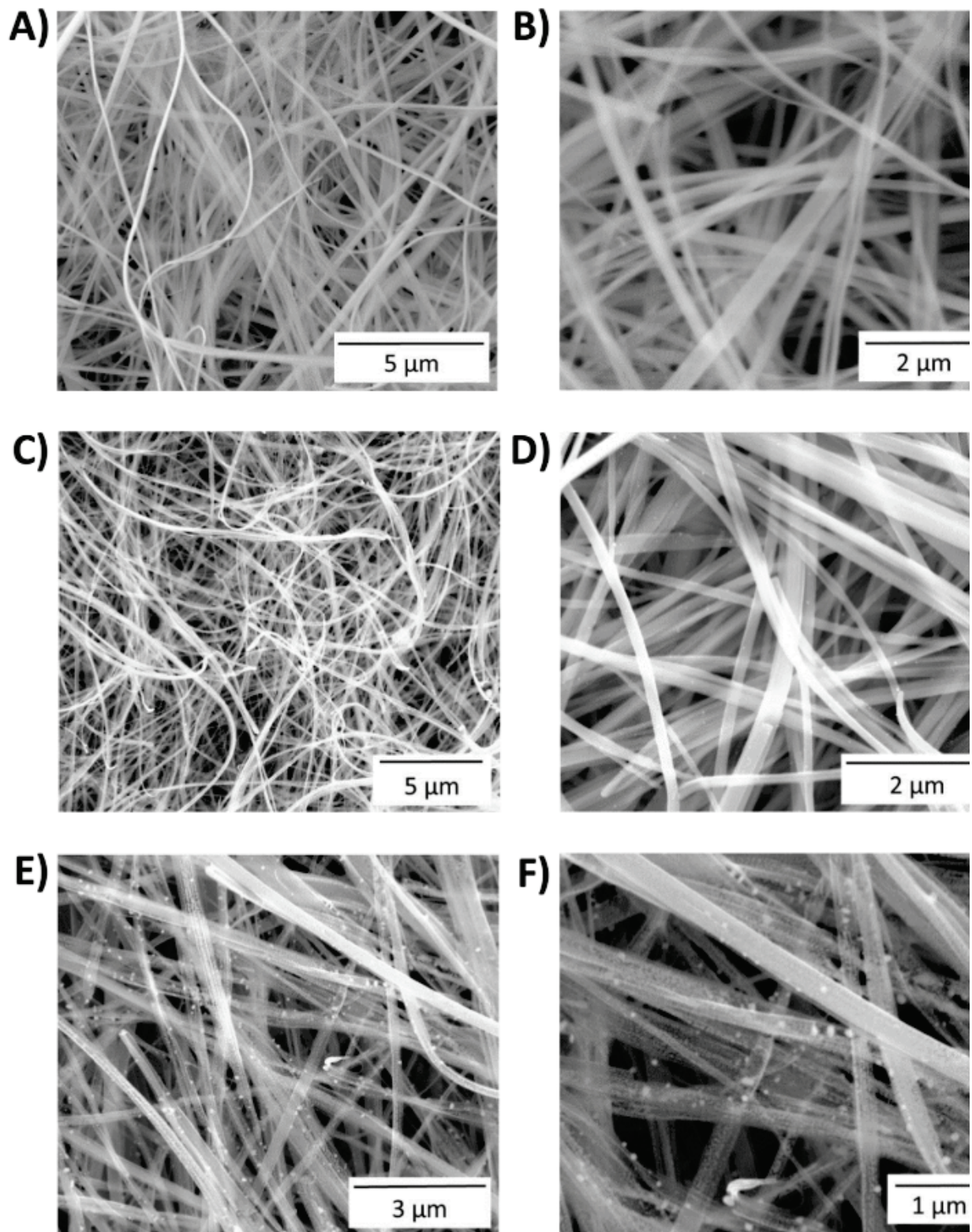
**Figure S11.** Histogram of the size distribution of the AuNPs formed on the  $[\text{Au}(\text{SPh})]_n$  fibers at 180 °C, 200 °C and 230 °C for 1 h. The diameters are measured from TEM images.



**Figure S12.** FTIR of the  $[\text{Au}(\text{SPh})]_n$  fibers calcined at different temperatures.



**Figure S13.** Remaining organic content after the calcinations at different temperatures and times of the  $[\text{Au}(\text{SPh})]_n$  fibers.



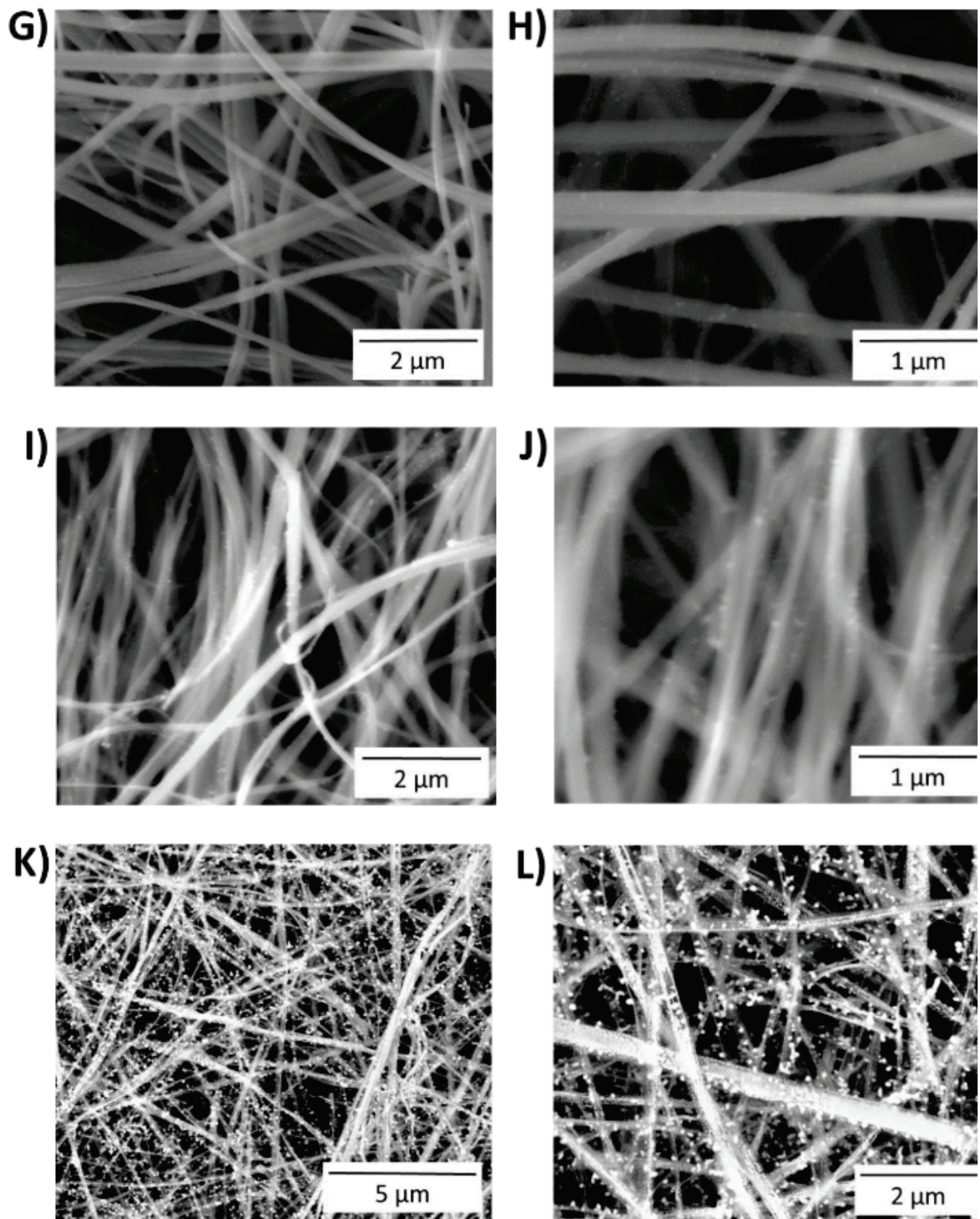


**Figure S14.** SEM images of the fibers calcined at the (A and B)  $180\text{ }^{\circ}\text{C} - 1\text{ h}$ , (C and D)  $180\text{ }^{\circ}\text{C} - 4\text{ h}$ , (E and F)  $180\text{ }^{\circ}\text{C} - 12\text{ h}$ , (G and H)  $200\text{ }^{\circ}\text{C} - 1\text{ h}$ , (I and J)  $200\text{ }^{\circ}\text{C} - 4\text{ h}$  and (K and L)  $200\text{ }^{\circ}\text{C} - 12\text{ h}$ .

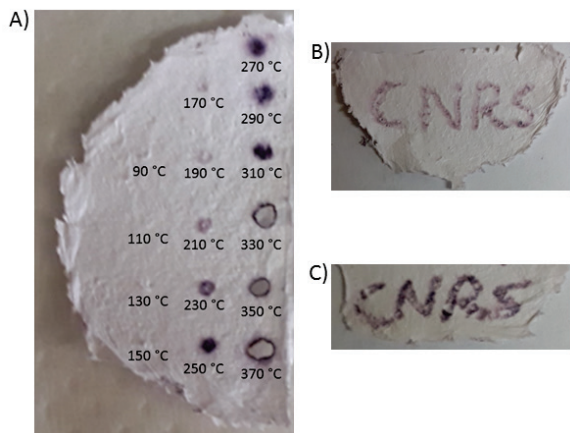


**Figure S15.** Photographs of marks left on the fibrous film after the contact with a soldering iron at A) different temperatures, B) 230 °C and C) 270 °C.

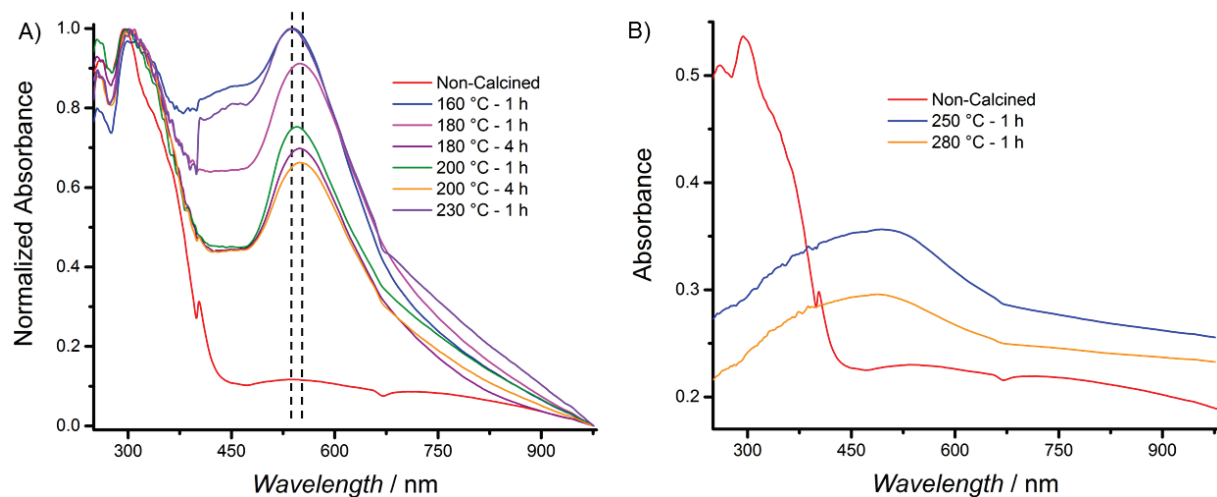


**Figure S16.** A) and B) UV-Vis spectra of the  $[\text{Au}(\text{SPh})]_n$  fibers heated at different temperatures and times.

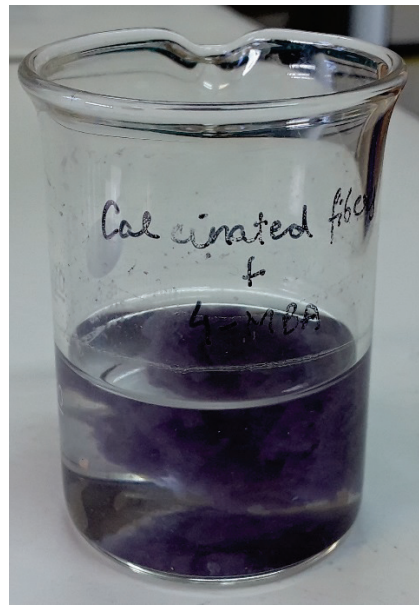


**Figure S17.** Photograph of the calcined fibers along with 4-MBA ( $1.25 \times 10^{-3}$  M) after studying the SERS effect. No leaching of the AuNPs can be seen clearly.

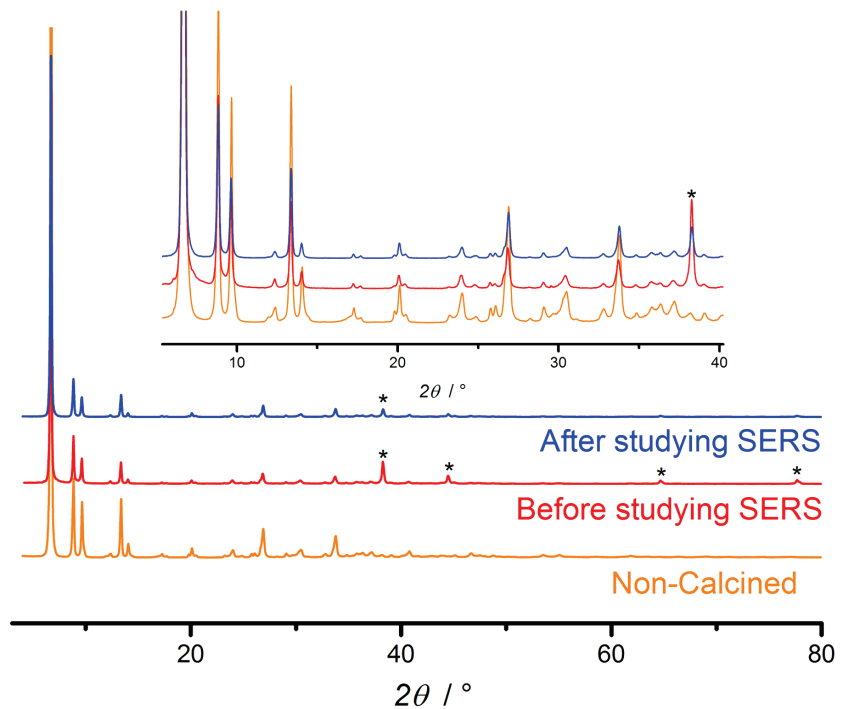


**Figure S18.** Comparison of the PXRD of the  $[Au(SPh)]_n$  fibers, the composite material obtained at  $230^\circ C$ -1h before and after the SERS effect study. The asterisks denote the FCC gold of the AuNPs.

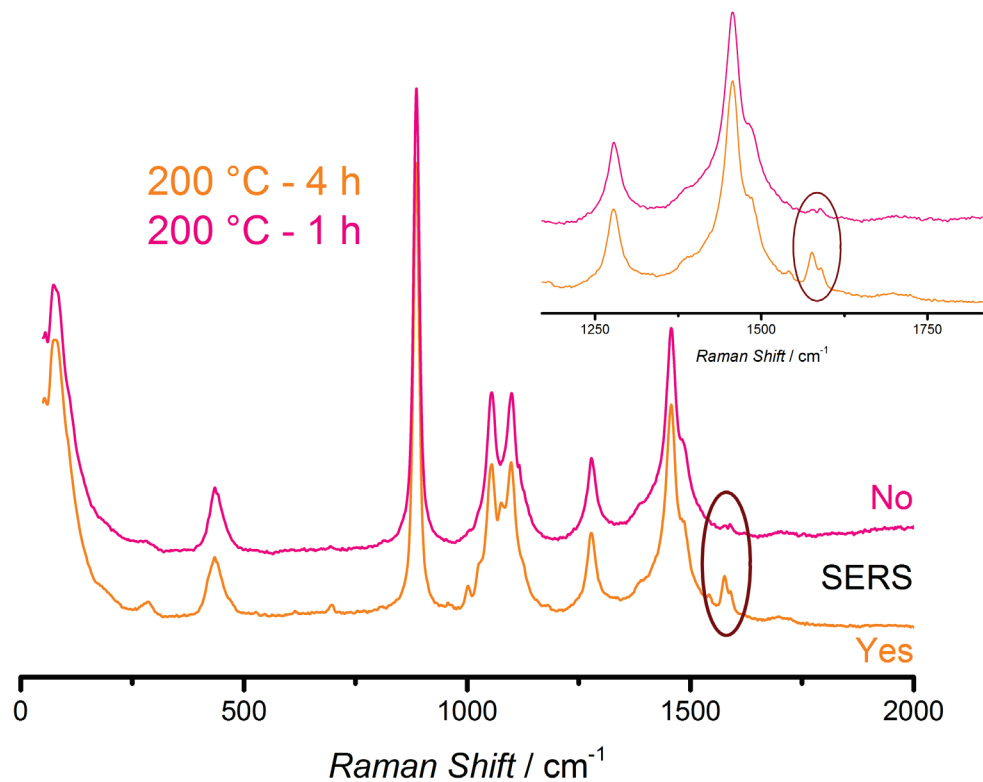


**Figure S19.** Comparison of the Raman spectra of the composite materials obtained after calcination of the fibers at 200 °C for 1 h and 4 h. The samples are mixed with 4-MBA (1.25 × 10<sup>-3</sup> M) to show the SERS effect.